Hindawi
Mathematical Problems in Engineering
Volume 2024, Article ID 2966138, 16 pages
https://doi.org/10.1155/2024/2966138

Research Article

Influence of the Hydraulic Circuit Setup on the Dynamic Performance of an Axial Piston Pump by Numerical and Experimental Analysis

Ala Eddin Chakroun, Mattia Battarra, and Emiliano Mucchi

Engineering Department Via G. Saragat, 1, University of Ferrara, Ferrara 44122, Italy

Correspondence should be addressed to Ala Eddin Chakroun; chakroun.ala.eddin@gmail.com

Received 29 August 2023; Revised 17 October 2023; Accepted 29 March 2024; Published 18 April 2024

Academic Editor: Antonio Forcina

The hydraulic circuit in hydraulic mechanisms may be the cause of several vibration anomalies. Flexible pipes, in particular, commonly used in test rigs, may be the source of vibration issues due to their relatively low natural frequencies altering the pump noise, vibration, and harshness (NVH) performance. The purpose of this study is to detail a methodology based on lumped parameter modeling and experiments to analyze the circuit NVH behavior. An experimental study is carried out on two pump designs to determine the outlet pressure fluctuation of various test rig configurations. Numerical simulations are also performed to simulate the actual behavior of the hydraulic system considering these different test configurations. The tests are carried out at a chosen frequency range with a hydraulic circuit configuration representing realistic layouts. In these situations, the hydraulic circuit layout can be the source of NVH anomalies. Realistic design solutions are proposed to modify the test rig NVH behavior in order to achieve a flat response throughout the desired working range.

1. Introduction

Throughout history, each new type of pump has been invented to meet a specific type of need. From the Greek inventions of Ctesibius' reciprocating pump and Archimedes' screw pump in 200 BC [1] to the Italian inventions of Francesco di Giorgio Martini's centrifugal pump [2] and Agostino Ramelli's sliding vane pump [3] between the XVth and XVIth centuries to the industrial revolution era of multiple introductions of multiple new types of pumps. Nowadays, the focus is no longer on introducing new designs, but on improving the characteristics of existing types by optimizing design and performance-related features. One of the main goals is to minimize noise, vibration, and harshness (NVH).

There are enormous studies in the literature on volumetric pump studies. The following are a few works focusing on the dynamic behavior of pumps, which is the main objective of this study. In Mucchi et al.'s [4–7] studies, the focus was on elastodynamic analysis of gear pumps investigating pressure, eccentricity, meshing, and experimental validation. Other studies include lumped parameter modeling of a gear pump [8] and analytical investigations of vane pumps [9]. Centrifugal pumps (particularly high-speed pumps) are focused on the study by Hao et al. [10], which focuses on hydraulic and structural design. The challenges mentioned are cavitation and excitation, with several design solutions introduced that improve efficiency. The importance of rapid and accurate diagnosis using on-line vibration monitoring was also emphasized. A 3D CFD study of a twin-screw pump is performed to finally determine that the circumference deviation is not the main contributor to the backflow rate, but that it is the flank deviation [11]. There are other research works in the literature discussing simulations and modeling of this type of gear (e.g., [12, 13]). Finite element analysis is frequently used in strength calculation of pumps, and the study of Cieślicki and Karpenko [14] is one example of the recent studies that used this approach. Finite element analysis is also performed to study the vibratory performance of peristaltic pumps [15, 16]. These studies are just a few examples of the large amount of research conducted by academics on the dynamic performance of hydraulic pumps.

The most common type of pumps used to achieve high pressure (more than 15 MPa) are piston pumps in general and axial piston pumps in particular. These pumps excel in providing high pressure without a notable decrease in their performance. Their manufacturing procedure is relatively simple with a comparatively high accuracy due to the cylindrical geometry of the displacement chamber. Nevertheless, this type of pump is less dependent on the flow rates of the corresponding operating pressure. Also, the main drawback of this system is that it emits a high amount of NVH. Several research studies have been carried out on this subject. In the study of Harrison and Edge [17], efforts are made to reduce flow ripple with a healthy damped check valve (HDCV) by preventing rapid switching action. In the study of Kim et al. [18], it is mentioned that the noise emitted by the pump is deeply related to both, the cylinder pressure variation and the outlet pressure pulsations. In the study of Ericson et al. [19], it is indicated that is also possible to reduce noise with nonuniform placement of pistons (i.e., pitch angle, cylinder ports' pitch angle, the radial displacement of the piston, and the radius of the piston). Seeniraj et al. [20] proposed an optimized configuration of using both, a precompression and decompression filter volumes in a valve plate that led to a huge reduction in the noise emitted. The study of Casoli et al. [21] presented an active-controlled pressure ripple by continuously changing the swash plate inclination. This solution proved to be effective in reducing the pressure ripple and evidently the system overall NVH performance. The latest research made focuses also on active control [22], dynamic modeling [23–26], and design optimizations [27–32].

The hydraulic circuit setup can also play a big role in the NVH performance of axial piston pumps. Some studies have focused on the relevance of having adequate geometry of suction ducts [33, 34]. Also, flow separation created by the change of the geometry of the flow path can lead to the generation of vortexes and turbulence in clearance volumes. Therefore, optimizations are made to improve streamlines of the flow in the suction duct. The study of Wang et al. [35] highlighted the fact that having a reservoir with a relatively large volume can maintain constant pressure when a wave of pressure reaches it. Pavić's [36] study highlighted the vibroacoustical behavior of different fluids flowing in different types of pipes (e.g., rigid and flexible). Studying the pressure fluctuation, a novel method of using a nonintrusive pressure sensors is introduced by Chevillotte et al. [37]. Conclusions are made by the same authors in a more recent study [38] that the pulsation wave plays a particular role in transporting most of the energy of the pressure pulsations through the pipe. The focus was also on the importance of the use of hybrid pipe analysis (i.e., combining measurements with model) to better understand the pipes dynamic features and, in particular, fluid–wall coupling. This will lead eventually to make particular changes to the design and size in order to improve the performance. In other studies [39, 40], the characterization and physical parameters of different fluids in a flow motion are determined using several introduced signal processing and acoustic analysis methods. Furthermore, with three transducers, three invariant functions can be determined. Using these functions, it is possible to derive the pressure spectrum, the velocity of the fluid flow, and the velocity of sound in the contained fluid. In a most recent study, Stosiak et al. [41] addressed an interesting topic of external mechanical vibrations causing excitation to a directional control valve in a heavy-duty military vehicle. The main conclusion mentions that a cushion made of a material with a high stiffness and damping mounted between the casing and the centering spring can lead to reduction of the vibration on the valve spool. In the review of Gao et al. [42], discussions are made regarding hydraulic circuits configurations and their influence on the vibration performance. Most of the review is focused on rigid pipes setups and passive and active control methods. It also highlights the work of Tuc [43] regarding the huge importance of flexible pipes in reducing the pressure fluctuations that are directly related to short length of the pipes at particular frequencies and long length of the pipes at broadband attenuation. The study of Grabbel and Ivantysynova [44] showed that displacement-controlled heavy duty actuators can be a competing solution to conventional valve-controlled systems considering their ability to allow sufficiently high dynamics. Therefore, not only pump design and control are the direct responsible on the vibration behavior of the mechanism, but the hydraulic circuit setup can have a great influence as well.

A review of the literature reveals a clear interest and a considerable number of studies on hydraulic pumps. This wide effort is explained by the massive need for better understanding and progress in this field of study. However, the research is usually focused on studying the machine rather than the test rig behavior, always described as constituted by rigid pipes. Nevertheless, the common practice in industry highlights the positive characteristics of flexible pipes related to their ease of use and their ability to smooth down pressure peaks. The main disadvantage of using flexible pipes is the relatively low natural frequency, which can cause resonances in low-frequency ranges. When this issue appears in test rigs, it makes the testing apparatus not appropriate for NVH evaluations, since it masks the actual behavior of the pump. On the basis of these observations, the present work details a methodology to assess the test rig NVH performance, providing insights regarding how the test rig may be modified to solve these issues. The proposed method takes advantage of a dedicated experimental campaign, where a variable displacement piston pump is used as source of pressure ripple and the attention is focused on the test rig response at the delivery line. Concurrently, a dedicated lumped parameter model of the system is adopted, detailing the model requirements that are necessary to achieve a robust assessment. The obtained model is validated against measured data and then it is shown how this tool may be used to achieve design solutions that improve the NVH characteristics of test rigs.

The work within the manuscript is organized as follows: Section 2 is dedicated to the description of the methodology. Section 3 provides a comprehensive overview of the measurement layout and experimental study, while in Section 4 the numerical modeling is described, considering the hydraulic circuit, the lumped parameter model, and the flexible pipe

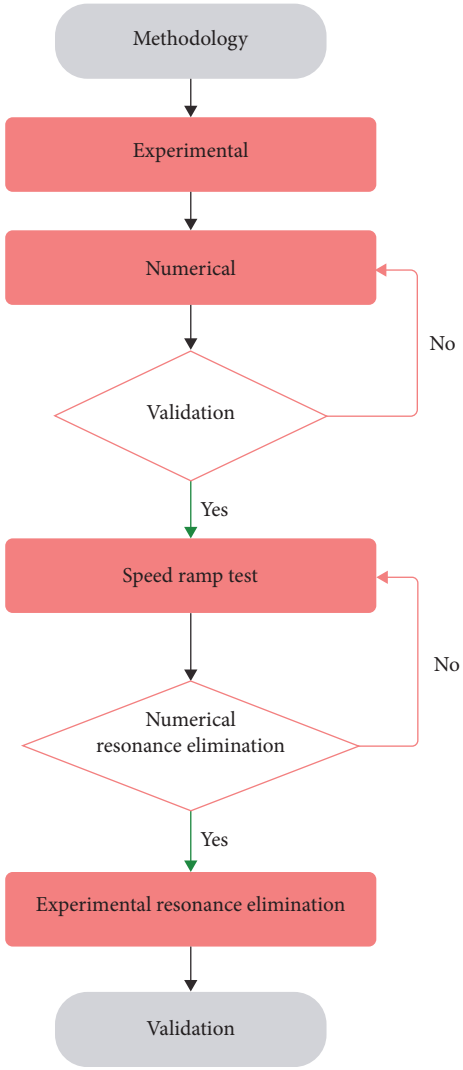

Figure 1: Flowchart of the methodology followed to achieve a resonance-free hydraulic circuit.

modeling method. In Section 5, the hydraulic layout is modeled with different methods to highlight that the accurate modeling of the circuit is required to achieve high levels of agreement with experiments. Afterward, the numerical model is used to deduce an improved layout free of resonances in the frequency of interest. The numerical results are therefore compared to the experimental ones throughout the different test configurations. The final results showed high accuracy for the different tested configurations. Finally, Section 6 is devoted to concluding remarks.

2. Methodology

This paper is devoted to the investigation of the influence of the hydraulic circuit layout on the NVH performance of a mechanism powered by an axial piston pump. The full methodology followed in this paper is summarized in the flowchart, as shown in Figure 1.

First, a dedicated test bench is designed and constructed to facilitate vibrational tests. The test bench is tailored to accommodate various components required for numerical simulations and experimental investigations. Careful attention is paid to the structural integrity, material properties, and mounting arrangements to ensure accurate data acquisition during the experiments.

A comprehensive numerical model is developed to simulate the experimental test bench. The numerical model is generated with a lumped parameter model that is built using Simcenter Amesim, to capture the physical behavior of the system accurately. The model is configured to incorporate the relevant parameters and boundary conditions of the experimental setup.

To ensure the accuracy and reliability of the numerical model, an iterative validation process is undertaken. The numerical predictions are continuously compared against experimental observations under different operating conditions. The model is refined and updated iteratively until a satisfactory agreement between the numerical and experimental results is achieved.

In order to analyze the system's response to varying operational speeds, speed ramp tests are conducted. These tests enabled the identification of potential resonance regions in the system. The insights gained from these tests are in the form of resonance detection and identification in order to be able to proceed with the resonance elimination solution.

A crucial step in achieving a resonance-free colormap is the introduction of a relatively short rigid pipe with different geometries at the outlet of the numerical model. Numerical simulations are performed with different short rigid pipe lengths to finally achieve a resonance-free colormap.

Upon successful identification of the resonance-free conditions through numerical simulations, the corresponding short rigid pipe, as deduced from the numerical investigations, is added to the outlet of the pump in the experimental test bench. This step aimed to replicate the resonance-free conditions obtained from the numerical simulations in the physical experimental setup.

The final step involved validating the experimental results obtained with the modified test bench against the desired resonance-free colormap. The validation process ensured that the modifications effectively eliminated resonances, leading to reliable and accurate test results.

3. Experimental Study

The present section describes the experimental study carried out to analyze the NVH behavior of a test rig built for this purpose. The tests are carried out by adopting two different variable displacement piston pumps to a realistic source of pressure ripple. The experimental setup of pump 1 is shown in Figure 2 where the outlet pipeline of the circuit is composed of pipe 1, load valve, and pipe 2.

The details of pump 1 are provided in Section 2. The experimental setup of this test configuration (Figure 2) is set to imitate an example of a realistic scenario. Where, regardless of the inlet pipe type, the outlet pipe setup is set as a flexible pipe (i.e., pipe 1) connected to a load valve connected to another flexible pipe (i.e., pipe 2) to finally

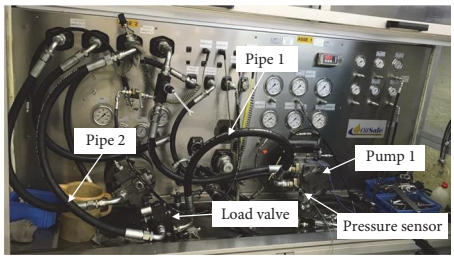

Figure 2: The test configuration of pump 1.

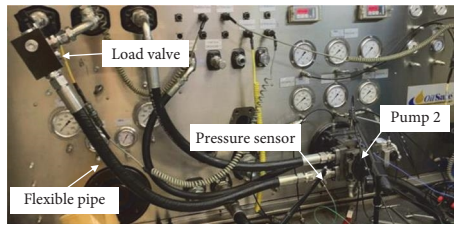

Figure 3: The test configuration of pump 2.

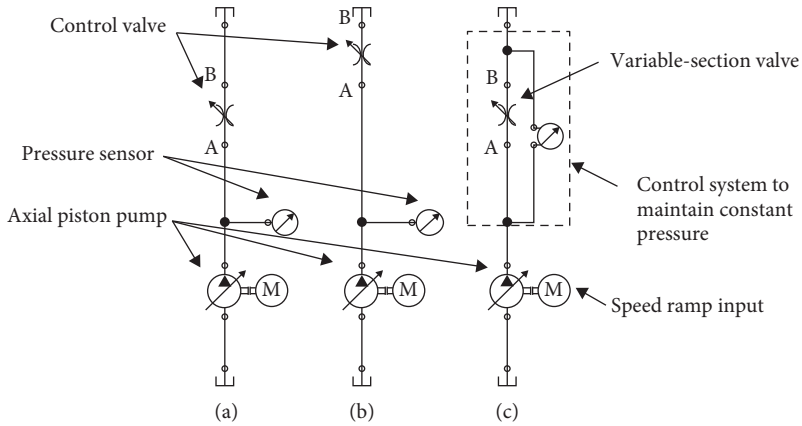

Figure 4: The schematic of the studied hydraulic circuits of pump 1 (a), pump 2 (b), and the speed ramp configuration (c).

circle back to the tank. The pressure fluctuation being studied is determined through a pressure sensor connected directly to the outlet of the pump.

The experimental setup of pump 2 is shown in Figure 3 where the outlet pipeline of the circuit is composed of a flexible pipe and a load valve. The details of pump 2 are provided in Section 2. Similar to the previous setup, this test configuration is also set to imitate another example of a realistic scenario. This time, the outlet flexible pipe is connected to the control valve that is directly connected to the tank. The pressure fluctuation being studied is also determined through a pressure sensor connected to the outlet of the pump.

The schematics of these test configurations are presented in Figures 4(a) and 4(b), respectively. Also, the schematic of speed ramp test is shown in Figure 4(c). The two circuits depicted in Figures 4(a) and 4(b) are set up in the same configuration, with a pressure sensor at the pump outlet followed by a control valve. The difference is that the former is set up with two flexible pipes before and after the control valve, while the latter is set up with a single flexible pipe before the control valve (i.e., at the pump outlet). In addition, the first scheme is used to test pump 1 and the second to test pump 2. The circuit shown in Figure 4(c) is set up with a control system to maintain a constant pressure. This system consists mainly of a variable-section valve controlled to achieve this objective.

4. Numerical Model

This section is devoted to detail the modeling procedure followed in this paper to simulate the different configurations of the hydraulic circuits. These models are established for pumps 1 and 2 with different piping layouts. Several methods used to model the flexible pipes are illustrated and the adequate configuration for the proposed situations is selected to be used for the resonance investigation. The lumped parameter model with its various components is also detailed. Subsequently, the estimation of the Young's modulus of the flexible pipe is also detailed.

4.1. Pump Modeling. The theoretical aspects of the studied pump are extensively detailed in the book of Ivantysyn and Ivantysynova [45] on hydraulic pumps and motors. The following part will give a brief explanation of the different geometrical and nongeometrical parameters of the studied machine. The study is made on two types of pumps, namely pump 1 and pump 2. These pumps are simulated with a lumped parameter model via Simcenter Amesim software. The simulation uses the approach of control volumes that are detailed in the book of Kalbfleisch and Ivantysynova [46]. Considering this approach, the evolution of the dynamic pressure p inside a control volume is written as follows [47]:

$$\frac{dp}{dt} = \frac{K}{V}\left(Q_r + Q_s - \frac{dV}{dt}\right), \tag{1}$$

where V, Q_r, and Q_s are the cylinder chamber fluid volume (i.e., control volume), flow rate, and volumetric losses (or external leakage), respectively. The latter is deduced considering the valve plate opening, gap between cylinder block and valve plate, and gap between piston and slipper. K is the fluid

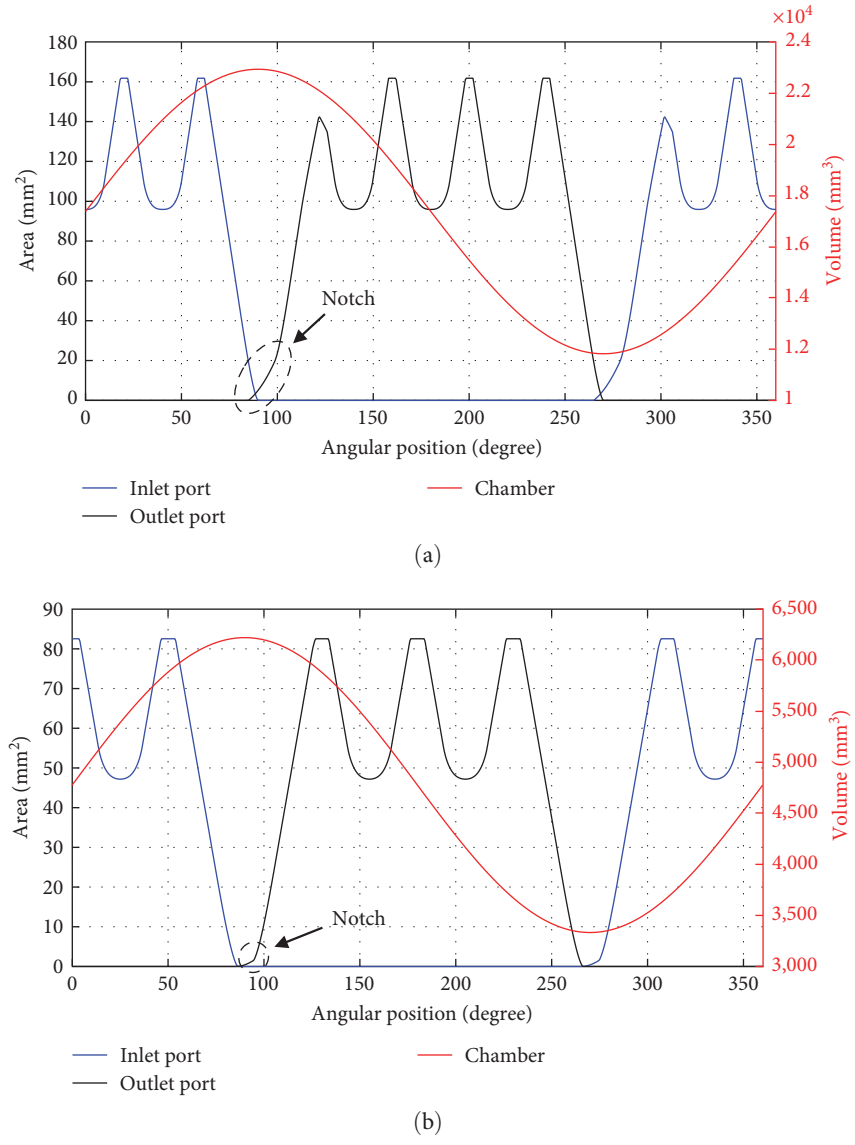

FIGURE 5: Inlet and outlet area variation, and chamber volume variation of pumps 1 (a) and 2 (b).

bulk modulus that depends on temperature and pressure characterizing the fluid resistance to compression. The interaction between the fluid (i.e., effective bulk temperature) and the flexible pipe wall (i.e., pipe wall stiffness) will influence significantly the vibrational performance of the hydraulic mechanism.

Despite the fact that the specific details of the piston pump components cannot be shared due to confidentiality restrictions, for the sake to give the reader a better understanding of the inlet and outlet volumetric exchange, the following details are provided. For pump 1, the swash plate has four segments in both inlet and outlet ports with a notch (i.e., pressure relief groove). For pump 2, the swash plate has three segments in both inlet and outlet ports as well. The geometry of the swash plates is determined directly from the real pump-designed CAD model. The contours of all segments including the notches are introduced in the lumped parameter model. The chamber volume variation is shown in Figure 5(a) for pump 1 and Figure 5(b) for pump 2.

The flow rate through an orifice is modeled by considering laminar, transitional, and turbulent flow variations. The expression used is written as follows:

$$Q = C_q A \sqrt{\frac{2|\Delta P|}{\rho}}, \tag{2}$$

where A is the opening area, ρ is the density, and ΔP is the pressure drop between the inner and outer ports of the orifice. The maximum coefficient C_q varies according to the law:

$$C_q = C_{q\max} \times \tanh\left(\frac{2\lambda}{\lambda_{\text{crit}}}\right). \tag{3}$$

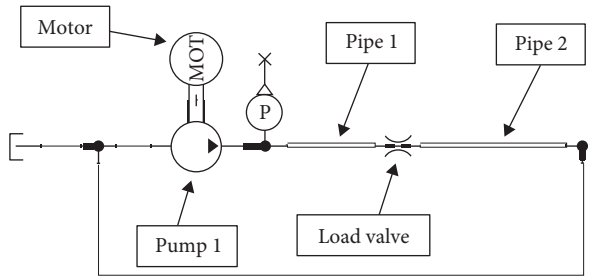

FIGURE 6: The hydraulic scheme of the test configuration of pump 1.

λ_{crit} indicates the flow transition from laminar to turbulent and λ is the flow number, defined as follows:

$$\lambda = \frac{d_h}{\nu}\sqrt{\frac{2|\Delta P|}{\rho}}, \tag{4}$$

where d_h is the hydraulic diameter and ν is the Poisson's ratio.

4.2. Test Rig Modeling. In order to properly simulate the experimental setup, the modeled piping layout of the hydraulic circuit of pump 1 (Figure 4(a)) is shown in Figure 6. The motor and pump 1 are modeled as a lumped parameter model detailed in Figure 7. The method used to model the flexible pipes (i.e., pipes 1 and 2) is explained in the next section. Similar to the experimental setup, the pressure sensor is set at the outlet of the pump.

Three methods are proposed to model the hydraulic circuit that is illustrated in Figure 8. The goal is to test different modeling methods of flexible pipes and observe their influence on the modeling accuracy. The different methods are tested for the hydraulic circuit of pump 1.

The first model configuration (Figure 8(a)) simulates pipes 1 and 2 as 2 volumetric chambers. The latter sets the pipe as constant volume at a corresponding pressure. The derivative pressure of the volumetric chamber is measured as follows:

$$\frac{dp_{\text{out}}}{dt} = \frac{B(p_{\text{out}})}{\text{vol}}\frac{\rho(p_0)}{\rho(p_{\text{out}})}(p_0 + p_{\text{out}}), \tag{5}$$

where ρ, p_0, and p_{out} are the corresponding density, the zero-pressure gauge, and the pressure of the oil at the outlet of the hydraulic chamber, respectively. B is the bulk modulus at the corresponding pressure and vol is the volume of the chamber. This method models the pipe without considering the effects related to the length of the circuit and the piping material properties.

The second model configuration (Figure 8(b)) replaces the volumetric chamber of pipe 1 with a 1D representation of the flexible piping. The concentrated parameter mathematical model transforms into a partial differential equation model, accurately depicting the pipe as a hydraulic transmission line. The last configuration (Figure 8(c)) models pipe 1 as a connection between a flexible pipe and two rigid conduits within its two limits. The rigid and flexible pipes are modeled with a distributed-parameter scheme of hydraulic pipes appropriate for scenarios where wave dynamics are assumed to have a significant impact. The inputs of this submodel are the wall thickness and Young's modulus of the corresponding pipe, since the actual bulk modulus of the fluid is computed by including the piping flexibility. The pressure derivatives between inlet and outlet of the pipe are computed as follows:

$$\frac{\partial P}{\partial t} = -\frac{A_c}{\beta_{\text{eff}}}\frac{\partial Q}{\partial x}, \tag{6}$$

where β_{eff} is the effective bulk modulus expressed as follows:

$$\beta_{\text{eff}} = \left(\frac{1}{\beta_{VG46}} + \frac{1}{B_p}\right)^{-1}, \tag{7}$$

where β_{VG46} is the bulk modulus of the hydraulic oil VG 46, which is the one adopted during the tests. The parameters of this oil are illustrated in Table 1. These parameters are considered for the oil at a constant temperature (60°C). The pipe's wall bulk modulus is expressed as follows:

$$\beta_p = \frac{1 + w_{\text{comp}}(p - p_0)}{w_{\text{comp}}}, \tag{8}$$

where p_0 and p are the pressures at the inlet and the outlet, respectively. Parameter w_{comp} is the wall compliance expressed as follows:

$$w_{\text{comp}} = \frac{2}{E_p}\left(\frac{r_o^2 + r_i^2}{r_o^2 - r_i^2} + \nu - \nu\frac{r_i^2}{r_o^2 - r_i^2}\right), \tag{9}$$

where r_o and r_i are the outer and the inner radii of the pipe. The hydraulic circuit model of the hydraulic scheme of pump 2 shown in Figure 4(b) is illustrated in Figure 9. The motor and pump 2 are also modeled according to the described lumped parameter model (Figure 7). Similar to the previous test setup, the pressure sensor is located at the outlet of the pump. The model is made respecting the schematic representation of the corresponding pump and motor (Figure 7). It is composed of an axial piston pump powered with an electric motor. The design parameters are directly implemented from the CAD model of the real pump. The most relevant physical aspects considered in the pump submodel are already detailed in Section 2.1. The pump consists of nine pistons placed in a circular pattern inside of a barrel. A shaft that is in alignment with the pistons causes the barrel to spin about its symmetry axis. Each piston's end contacts the swash plate with the aid of a slipper (Figure 7).

The swash plate angle offset from the orthogonal axis of the shaft must be greater than zero in order to pump the fluid. As a result, each piston glides up and down inside of its sleeve, bringing fluid from the intake port into the piston

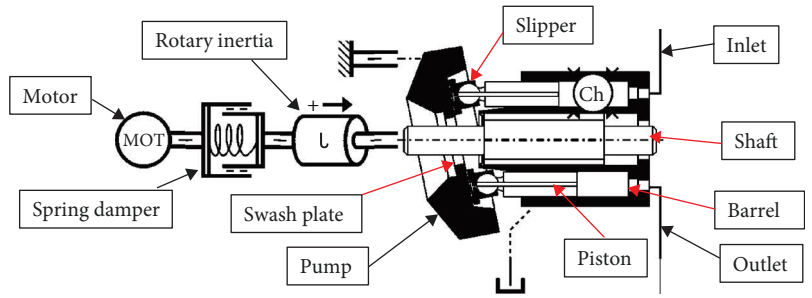

FIGURE 7: Axial piston pump lumped parameter model.

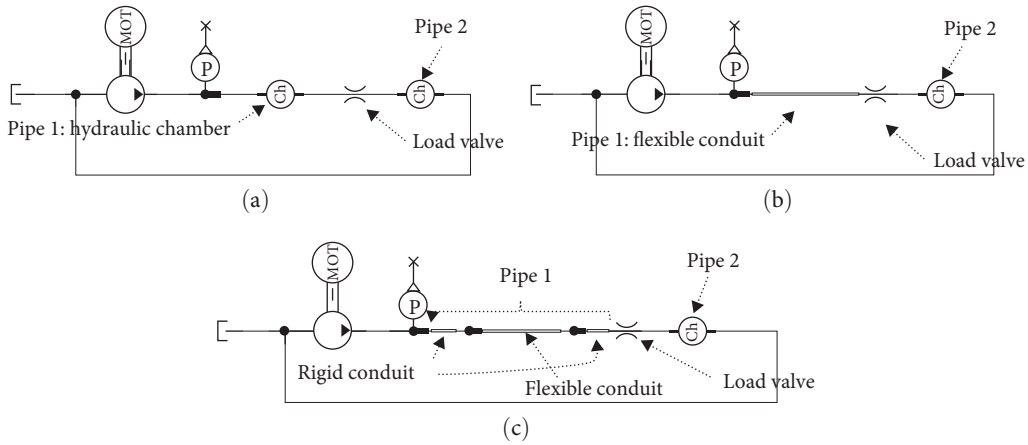

FIGURE 8: First (a), second (b), and third (c) model configurations.

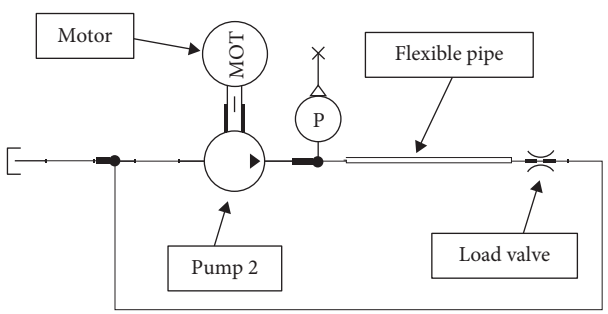

FIGURE 9: The hydraulic scheme of the test configuration of pump 2.

chamber and releasing it via the outlet port. Every rotation of the piston defines one full pumping cycle, which is defined by this procedure. All geometrical details are introduced in the pump model including pistons, swash plate, and valve plate. The valve plate of pump 1 has a 4×4 inlet and outlet segments, while that of pump 1 has 3×3 segments. Leakages are considered at the port plate, barrels, and slippers. The dynamics of the pump is modeled with a rotary spring damper and a rotary inertia, as shown in Figure 7.

The spring dumper is characterized with a stiffness K_d and a damper rating C_d. The submodel has two ports, and at each of them, a torque is set as output. Rotary velocities in rev/min must be provided as inputs. A state variable is used to determine the twist angle in degrees. The rotary inertia J is determined from the rotating components, such as shaft, cylinder block, ring, pistons, and slippers. This two-port submodel is characterized by two external torques. The angular displacement in degrees and the rotating velocity in rev/min are computed by the submodel and set as outputs. By including end stops, the angular displacement may be constrained to a particular range.

When speed run-up tests are concerned, the main challenge is the calibration of the flow rate as a function of pressure to maintain a constant mean value of the outlet pressure. This calibration work is performed on the efflux coefficients describing the flow rate as a function of pressure through an orifice resulted in a nonsignificant change in the dynamic pressure. The submodel used to fulfill this calibration functions as a systematic variable orifice. It is set with the geometry of the orifice and the flow rate coefficient as inputs.

The hydraulic pipe used in hydraulic circuits is made with layers of different materials. It is composed of a tube and a cover made of synthetic nitrile rubber and synthetic rubber resistant to abrasion and ozone, respectively. Four layers of high tensile steel wire are present between the tube and the cover. It is very complicated to model the exact behavior of this kind of pipes made of several materials. However, it is proposed to use an approximated Young's modulus. In the study of Dudziński and Skurjat [48], the bulk modulus of a flexible pipe with a 16 mm diameter and two layers of high tensile steel wire (i.e., DN16, 2SN) was investigated for multiple pressure values. Moreover, three

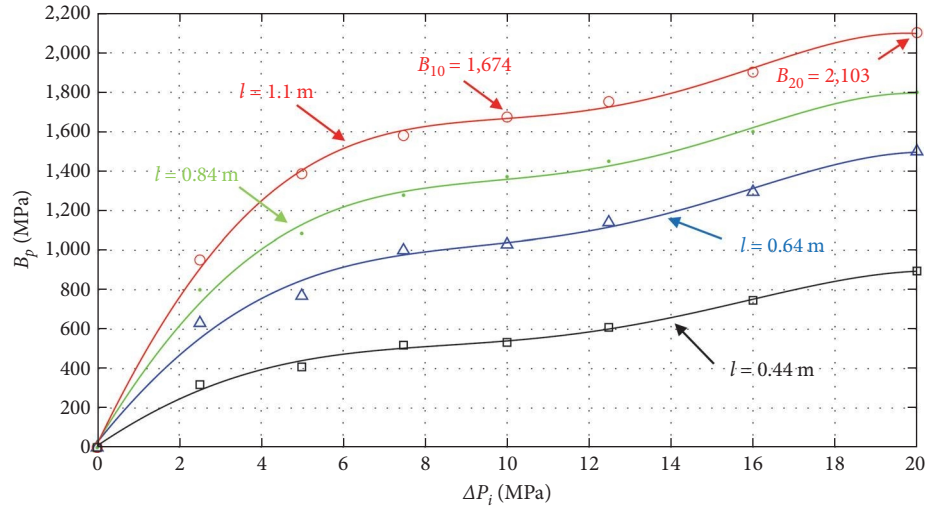

FIGURE 10: The bulk modulus of 0.44, 0.64, and 0.84 m DN16, 2SN flexible pipe of tests made in the study of Dudziński and Skurjat [48] with an estimated prolongation to 20 MPa and the estimated curve of 1.1 m pipe.

lengths of 0.44, 0.64, and 0.84 m at 20°C have been tested (Figure 10).

To determine the curve of a 1.1 m long pipe, it is proposed to predict it based on the mentioned three tests. The estimated curve is shown in Figure 10. From this curve, the bulk modulus of 1.1 m long DN16, 2SN pipe is determined for both pressures of 10 and 20 MPa. The Young's modulus is therefore determined using the following equation:

$$E = 3B_p(1 - 2\nu). \tag{10}$$

The flexible pipe used in this paper for both pumps configurations is a DN25, 4SN. To do the approximation of the Young's modulus of this pipe, a factor corresponding to the diameter difference (x25/16), a factor corresponding to the number of steel wire layers (x2), and a factor corresponding to temperature (x1.4) are applied. The value of the estimated Young's modulus for the pressure of 10 MPa and for 20 MPa are therefore determined.

5. Numerical–Experimental Results Comparison

The mentioned suggestions to model the pipes (Figure 8) are tested here and compared to the real experimental signals. The pump used in these tests is pump 1, and the pressure fluctuation is calculated throughout these simulations. Tests are made at a pressure of 100 bar and speeds of 1,200, 1,600, and 2,200 RPM. The characteristics of the pumps and the value of the parameters considered in the model are shown in Table 1. In the numerical model, the temperature of the fluid is considered constant (at 60°C) as the results are determined at the stationary regime. Also, the temperature of the pipe is estimated to be equal to the temperature of the fluid. In the experimental test, both a cooling and a heating system are used to maintain a constant oil temperature. The former takes the form of a liquid–air heat exchanger that reduces the oil temperature when necessary. The latter is a resistance system that is submerged in the oil to reheat it when the oil temperature falls below the desired limit. Both systems are monitored by a thermostat that guarantees a temperature of 60 ± 2°C.

The numerical and experimental results made with the first model configuration (Figure 8(a)) are shown in Figure 11. Differences in the amplitude can be clearly seen in both time and frequency domain. Regardless of the accurate modeling of the pump set with the lumped parameter model, the numerical results show a noticeable inaccuracy with the experimental ones. The use of the 0D approach based on a single volumetric chamber as a model for the flexible pipe is clearly inadequate in the current situation, since it is not capable to represent the dynamics of the circuit. As a matter of fact, the test rig is altering the pump delivery fluctuations by means of a transfer function that depends on the geometry of the circuit itself.

In order to overcome the highlighted limitations, the model is improved by including the pipe as a long, flexible conduit, including the theoretical aspects that consider the dynamics of a flowing fluid withing the pipe (detailed in Section 3). Consequently, the volumetric chamber of pipe 1 (Figure 8(a)) is substituted by a pipe featuring the geometric details of the actual pipe (i.e., diameter, thickness, material, etc.). The numerical results of this model (Figure 8(b)) are compared to the experimental results and are shown in Figure 12.

The use of this model (i.e., Figure 8(b)) improves the accuracy of the estimations achieved in Figure 8(a). The pressure fluctuation is showing a better correlation with experimental signals. The amplitude values in the spectra are closer to the real signal but still show significant inaccuracies. It can be concluded here that with an accurate model of the pump and the long piping approach, the correlation between numerical and experimental results is still not sufficiently consistent, especially for 2,200 rpm. This is suggested to be the result of having the rigid connections at both limits

Table 1: The pumps characteristics and the model parameters.

Parameters	Pump 1	Pump 2
The rotary inertia, J (kg·m^3)	15.48×10^{-3}	12.92×10^{-3}
Spring damper stiffness, K_d (Nm/rad)	125×10^3	26.4×10^3
Weight (kg)	55	28.8
Nominal displacement (cm^3/rev)	100	34
Continuous pressure (bar)	400	300
Swash plate angle (degree)	16.5	18
Rotational speed limits (RPM)	500–3, 000	500–3, 800
Spring damper damping, C_d (Nm/(rad/s))	8.8	
Number of pistons	9	
The speed of sound in a hydraulic oil, c_0 (m/s)	1, 461	
The cross-section of the flexible pipe, A (cm^2)	530.93	
Length of pipe 1, l (m)	1.1	
Volume of pipe 2, V (cm^3)	214.82	
The maximum coefficient, C_q	0.7	
Resonance frequency, f (Hz)	365	
Estimated Young's modulus at 100 bar (MPa)	8, 881.5	
Estimated Young's modulus at 200 bar (MPa)	9, 155.9	
Density of VG 46 (kg/m^3)	845.65	
Bulk modulus of VG at 100 bar gauge (MPa)	1, 351.38	
Bulk modulus of VG at 200 bar gauge (MPa)	1, 459	
Bulk modulus of VG at 300 bar gauge (MPa)	1, 565.82	
Viscosity of VG at 100 bar gauge (cP)	127.62	
Viscosity of VG at 200 bar gauge (cP)	129.45	
Viscosity of VG at 300 bar gauge (cP)	131.17	

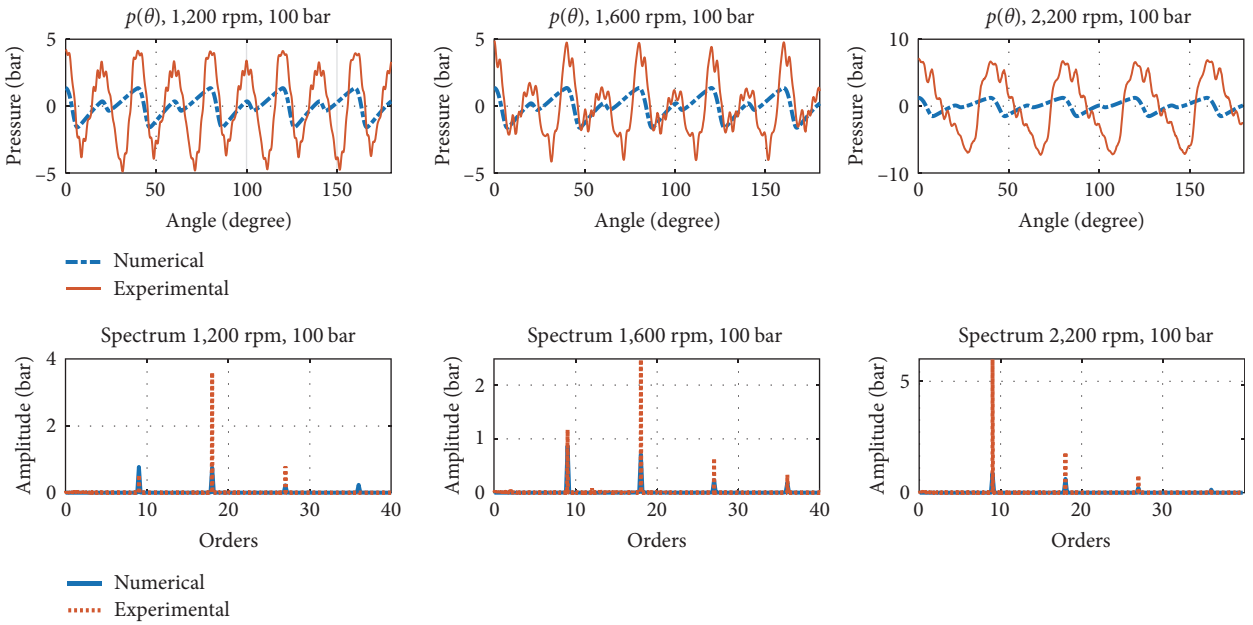

Figure 11: Numerical and experimental comparison of pressure fluctuation and spectrum of all tested speed configurations for 100 bar of the first model configuration.

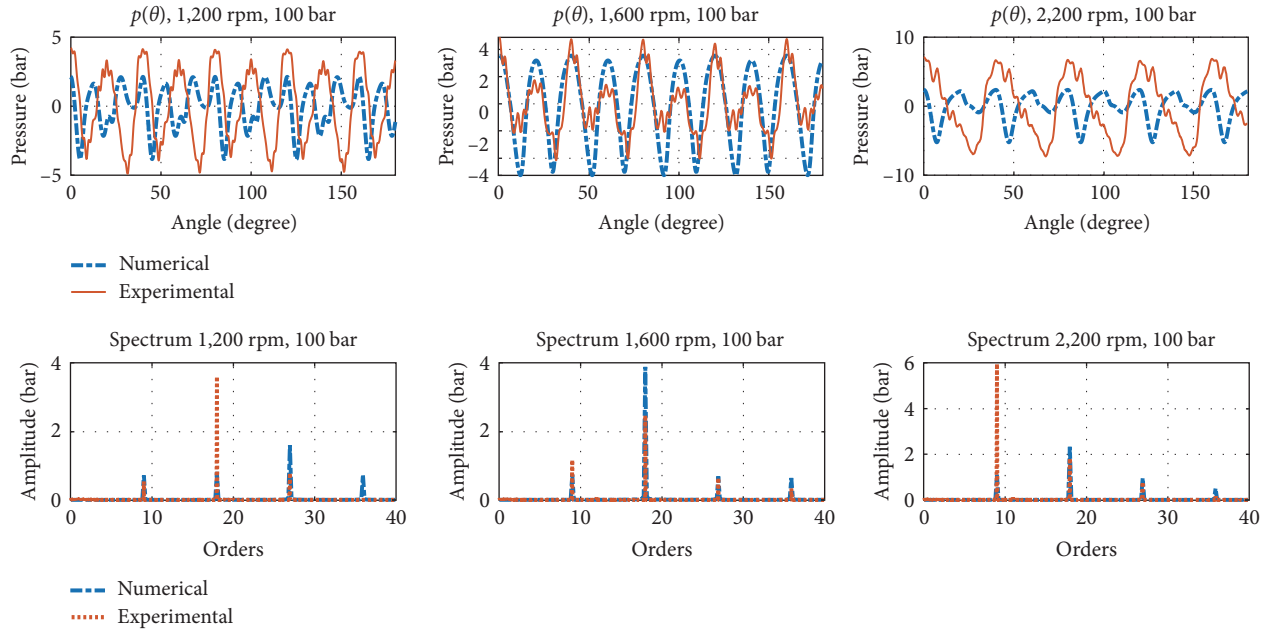

Figure 12: Numerical and experimental comparison of pressure fluctuation and spectrum of all tested speed configurations for 100 bar of the second model configuration.

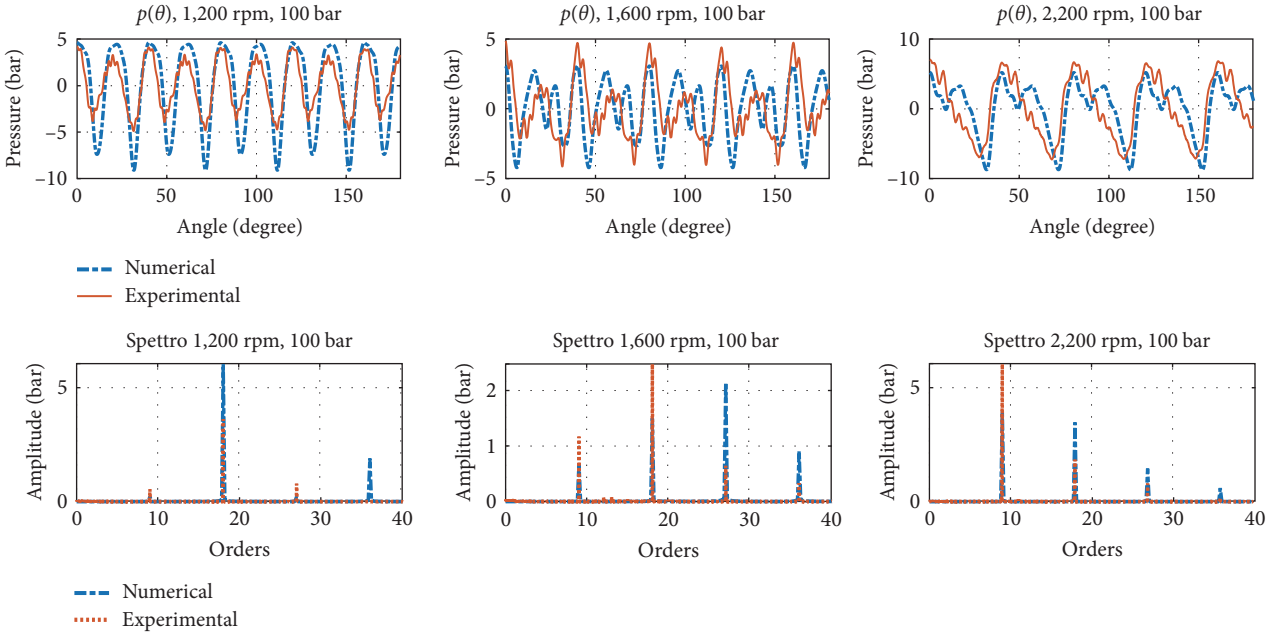

Figure 13: Numerical and experimental comparison of pressure fluctuation and spectrum of all tested speed configurations for 100 bar of the third model configuration.

of the flexible pipe which also have their own influence on the dynamic behavior of the circuit. This issue is therefore taken into account in the following model.

The following model (i.e., Figure 8(c)) simulates the flexible pipe as mentioned, with two short rigid pipes connected at the limits of a flexible pipe. The aim is to observe whether or not the two small rigid connections influence the behavior of the hydraulic circuit. The numerical results are therefore compared with the experimental ones and are shown in Figure 13.

The results show similarities between numerical and experimental signals. The method proposed in this model (i.e., Figure 8(c)) is highly accurate compared to the two previous models. The simulation improved with better modeling of the outlet pipe, particularly for the high-speed configuration.

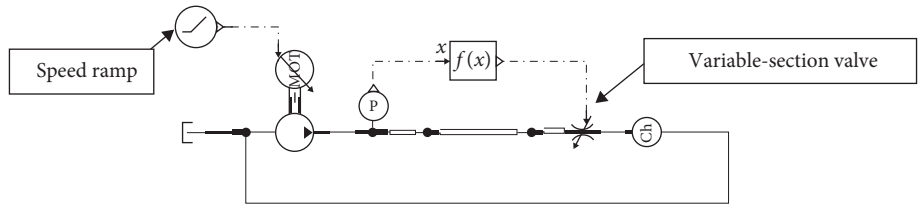

Figure 14: Rump test simulation model.

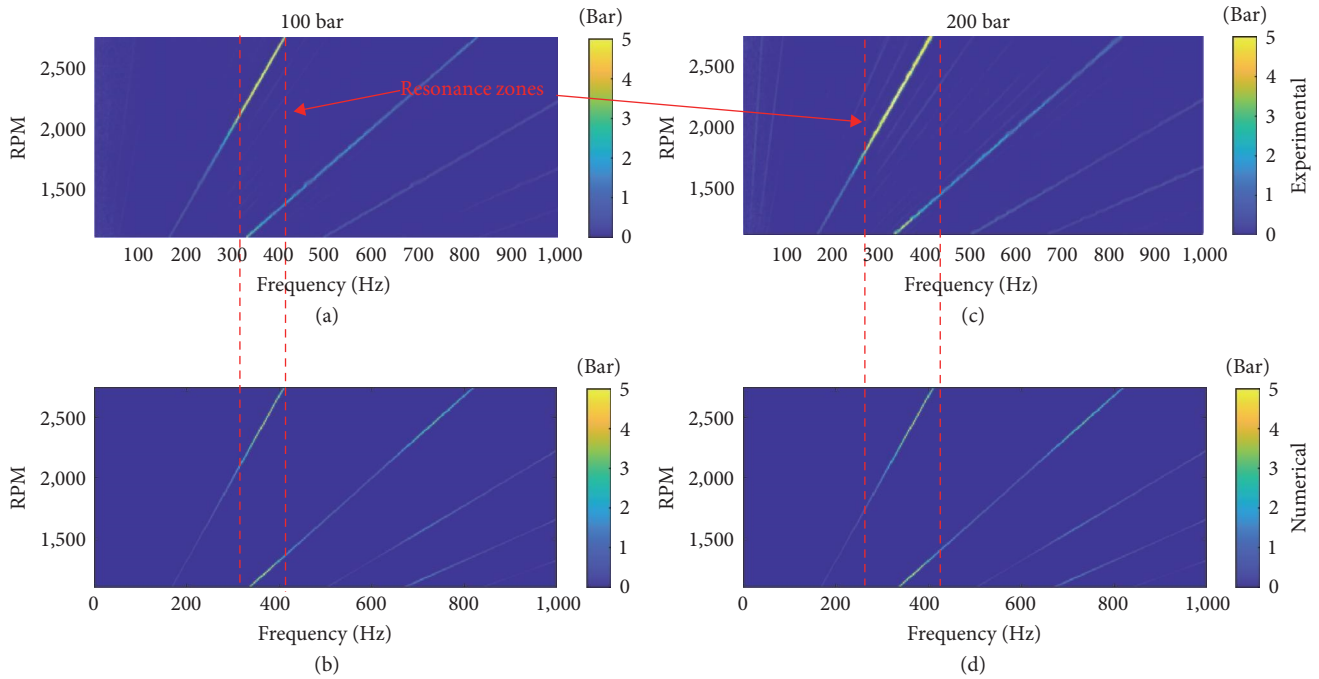

Figure 15: Experimental (100 bar (a) and 200 bar (c)) and numerical (100 bar (b) and 200 bar (d)) speed ramp (1,000–2,800 rpm) test of pump 1.

Regardless of the accurate modeling of the pump, it is necessary to proceed with the last proposed modeling method being the method with the best accuracy for the situation being studied. This is also because the following investigation consists of observing resonances in a studied frequency range. With resonances, the influence of interaction between the fluid flow and the piping system is significant. The next step is to observe the resonances caused by the use of flexible pipes and to propose a solution to move these resonances out of the studied frequency range.

Experimental tests are set up to simulate real-time scenarios with the piping layout already mentioned. It is decided to carry out speed ramp tests to observe NVH anomalies. The corresponding numerical models are then simulated and compared with the experimental ones. A solution is finally proposed to shift the resonances encountered, observed in the color map spectra, out of the frequency range studied. The simulation model of this speed ramp test is shown in Figure 14 (for the corresponding pump).

The test is made using pump 1 where the speed is varied from 1,000 to 2,800 RPM for pressures of 100 and 200 bar. To keep the pressure variation constant, it is proposed to use a variable-section valve, driven by a control system. Eventually, the experimental and numerical colormaps of the tests are plotted in Figure 15.

The numerical and experimental signals agree with resonances zones in the vicinity of the resonance frequency f for the pressures of 100 bar (at (350 400) Hz) and for 200 bar (at (290 410)). As it can also be noticed that the amplitude and size of the resonance zone increase with the increase of pressure.

The outlet flexible pipe is modeled in the test configuration of pump 2 similarly to pump 1. The speed is varied from 1,000 to 2,800 RPM for pressures of 100 and 300 bar for this case. The Young's modulus ($E_{300} = 9,438.8$ MPa) of the pipe at 300 bar is estimated in the same mentioned procedure in Section 3. The results of speed rump tests are shown in Figure 16.

The numerical and experimental signals agree as well with the frequencies of the resonance zones for the pressures of 100 bar (at (350 460) Hz) and 300 bar (at (350 480) Hz). The same observation is made here where the amplitude and the size of the resonance zone increase with the increase of pressure.

In order to shift the resonances out of the studied frequency range (i.e., shift them to a higher frequency), it is proposed to add a short rigid pipe between the pump outlet and the flexible pipe. This is proposed knowing that short rigid pipes have a relatively high natural frequency.

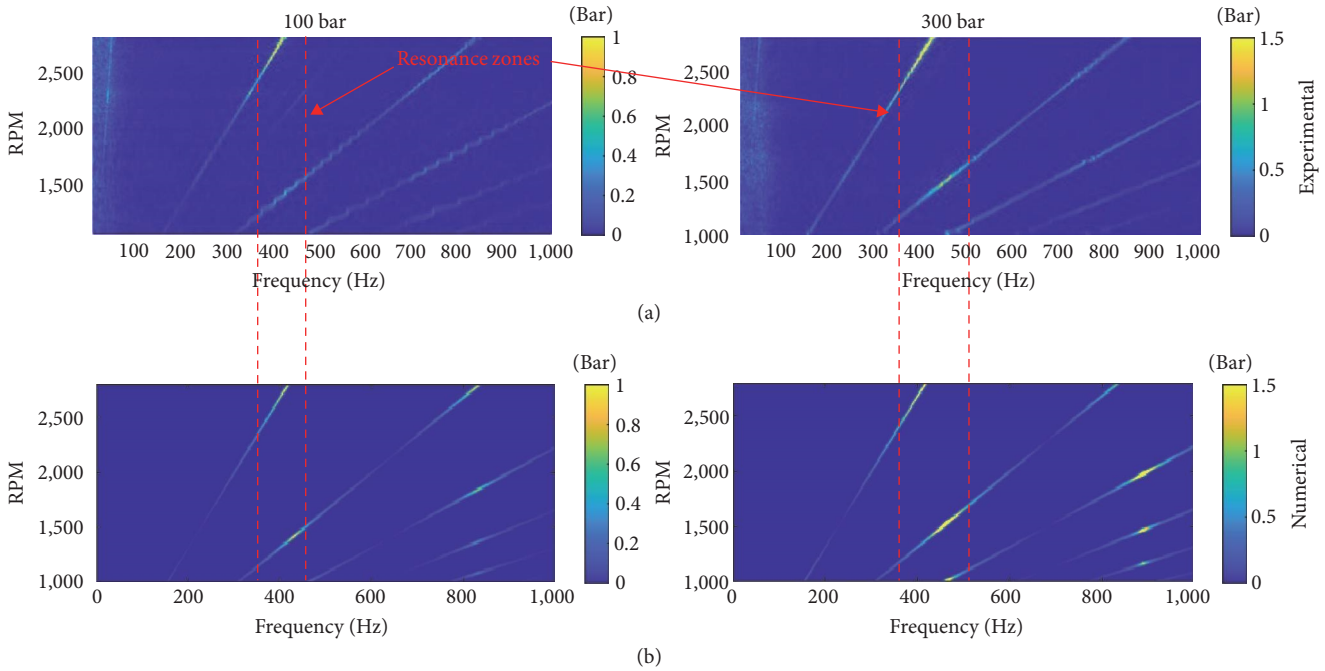

Figure 16: Experimental (a) and numerical (b) speed ramp (1,000–2,800 rpm) test for 100 and 300 bar of pump 2.

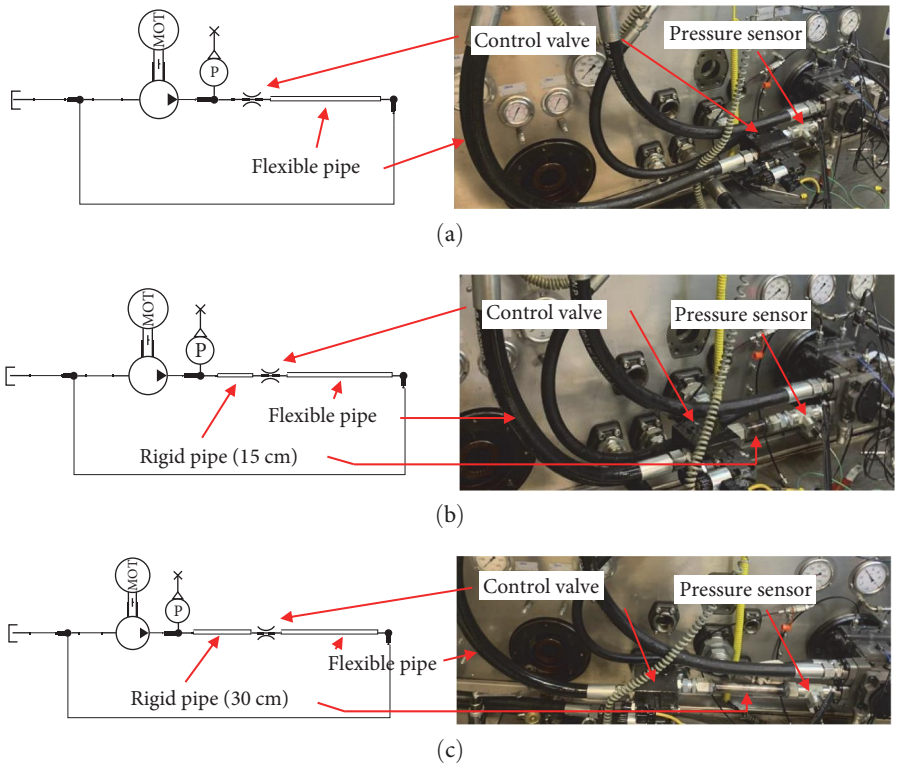

Figure 17: First (a), second (b), and third (c) tested configurations.

Numerical tests are carried out to find the optimal solution. Afterward, the solutions are tested experimentally to confirm their adequacy. The optimal solutions are tested at 100 and 300 bar of three configurations of pump 2:

(i) First configuration: The control valve is directly connected to the pressure sensor at the outlet (Figure 17(a)).

(ii) Second configuration: A rigid pipe at the outlet before the control valve and the flexible pipe (Figure 17(b)).

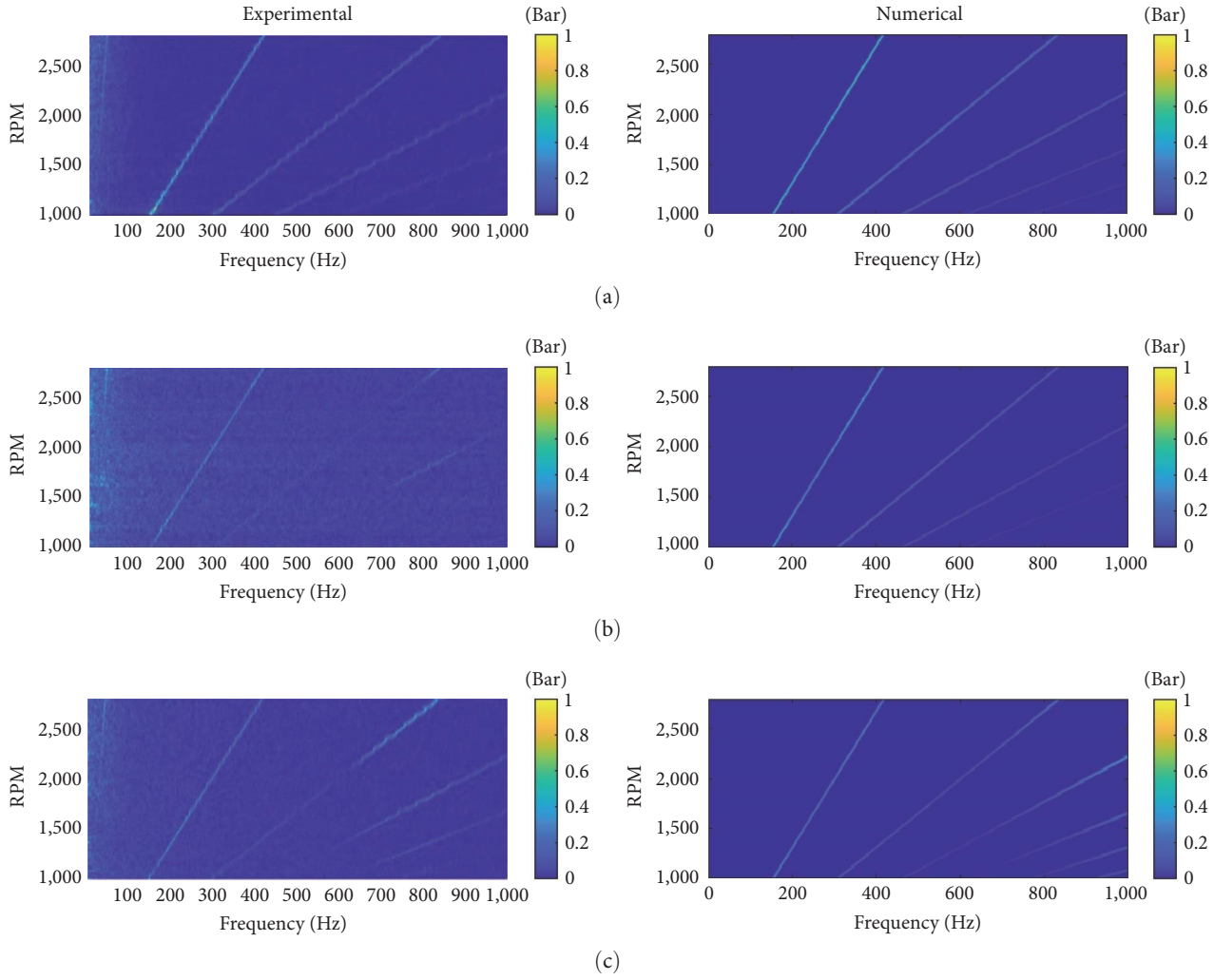

Figure 18: Color map of the first (a), second (b), and third (c) test configuration at 100 bar.

(iii) Third configuration: A longer rigid pipe at the outlet before the control valve and the flexible pipe (Figure 17(c)).

The three configurations are tested numerically and experimentally, and the results are compared in Figure 18. The three configurations behave similarly, with the first harmonic having the highest amplitudes. The first configuration has a slightly higher pressure amplitude at the first harmonic than the other two. This amplitude is reduced by using a rigid pipe (i.e., configuration 2) at the pump outlet. It is further reduced by using a longer rigid pipe (i.e., configuration 3). It is clearly seen that there is no occurrence of resonances in the three configurations.

The pressure sensor is acting here as a short rigid pipe itself (Figure 17(a)). Configuration 3 showed the lowest amplitudes of the harmonics to be the solution with the best NVH performance. Longer rigid pipes can result in the occurrence of new resonances. Therefore, configuration 3 can be selected as the optimum solution among the configurations tested. Ultimately, all the proposed solutions succeeded in achieving a resonance-free hydraulic system in the studied frequency range.

To verify the sensitivity of the proposed solution to pressure, the same tests are performed at a higher pressure of 300 bar. The numerical and experimental results are therefore compared and are shown in Figure 19. Similar to the 100 bar tests, all three configurations have consistent behavior, with the first harmonic showing the highest amplitudes. Also, the amplitude is slightly reduced with the use of a longer rigid pipe at the outlet. The main observation is that there is no occurrence of resonances similarly to the tests of 100 bar pressure. This observation confirms the adequacy of the proposed solutions to shift resonances out of the studied frequency range for different pressures. It can also be confirmed that the third configuration is the optimal solution with the best NVH performance of the proposed solutions.

With the observation made for these three configurations at 100 and 300 bar that there is no occurrence of resonances, the solution has finally been confirmed adequate for different pressures. The addition of a relatively short rigid pipe in the outlet leads to the suppression of resonances (i.e., shift them

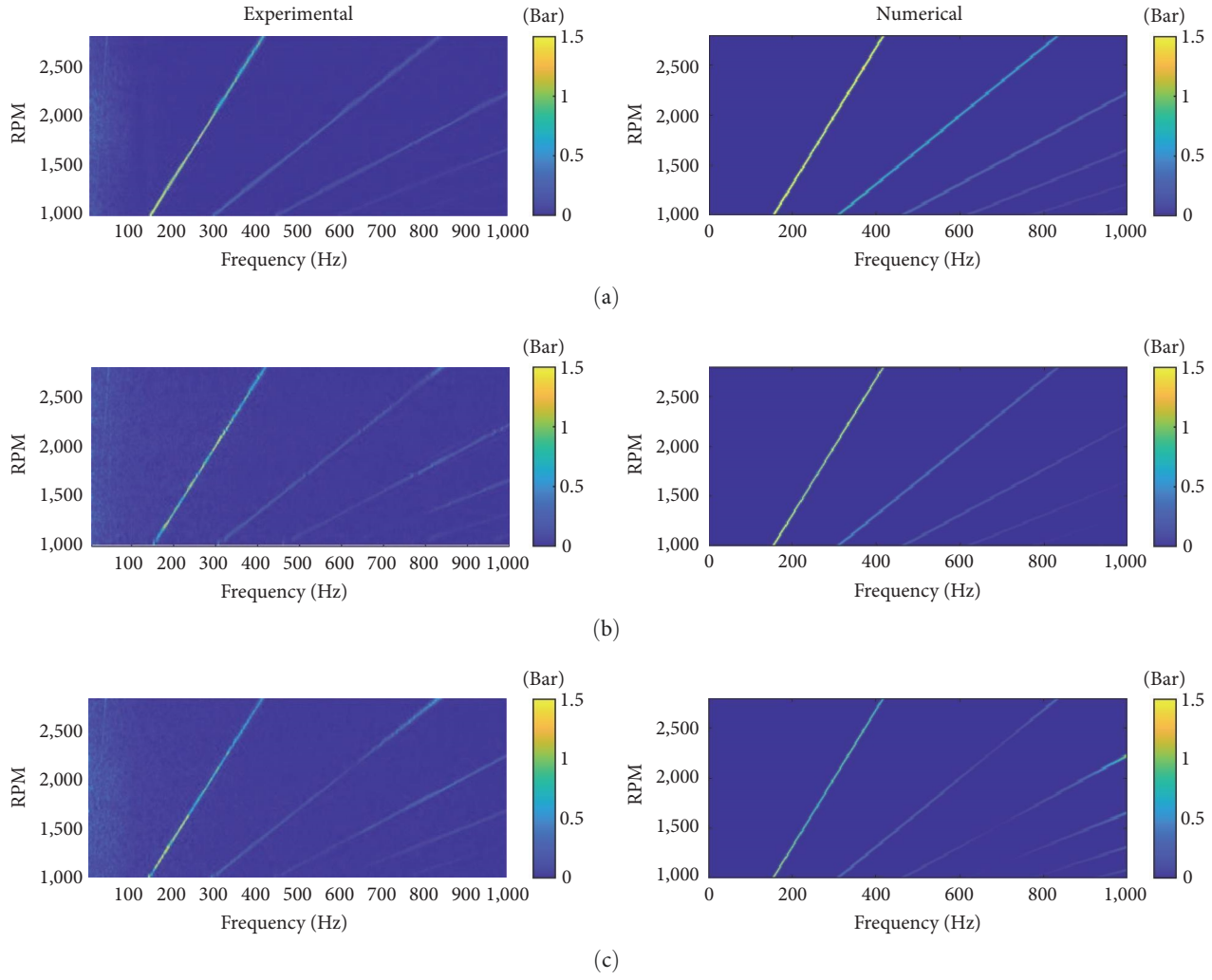

Figure 19: Color map of the first (a), second (b), and third (c) test configuration at 300 bar.

out of the studied frequency range) resulting from the use of flexible pipes. Ultimately, this solution improves the NVH performance of the entire hydraulic system.

6. Conclusion

The proposed study examined the influence of the type of pipes used in a hydraulic system on its dynamic performance. Hypotheses are first formulated to model the behavior of flexible pipes. The four layers of steel wire covered by two layers of rubber are modeled with an estimated Young's modulus. This estimation was sufficient to obtain accurate results, but more precise modeling would further improve the level of accuracy of the numerical–experimental comparison.

The use of an accurate lumped parameter model to simulate the behavior of axial piston pumps showed to be not sufficient when the outlet pipes were modeled as volumetric chambers. This is explained by the high importance of the accuracy of modeling the flexible pipes when there is dynamic interaction between the oil and the pipe regardless of how accurate the pump model is. Therefore, the solution proceeded in this paper is to model the flexible pipe at the outlet of the pump with the estimated Young's modulus with two relatively short rigid connections at both its limits.

Using this modeling procedure, speed ramp tests are caried out. The speed is varied from 1,000 to 2,800 RPM for pressures of 100 and 200 bar for pump 1 and for pressures of 100 and 300 bar for pump 2. The goal here is to observe examples of hydraulic layouts of realistic situations where NVH is relatively high. It is observed from the numerical–experimental comparison that the resonances appearing in the experimental colormaps are accurately appearing in the numerical colormaps, considering their frequency ranges and amplitudes. These resonances increase in both frequency range and amplitude with increasing pressure.

To improve the NVH performance of hydraulic circuits, the solution proposed in this paper is to exclude resonances from the frequency range of interest with adding a relatively short rigid pipe to the pump outlet. With this solution, the color maps showed no appearance of resonances at the

studied frequency range for the different tested configurations. Additionally, the amplitude of the harmonics decreases as the length of the rigid pipe increases. Therefore, the optimal length of the added rigid pipes is 30 cm for the studied hydraulic circuit. Consequently, this type of study can be carried out to obtain resonance-free hydraulic circuits by adding a relatively short rigid pipe to the outlet of the pump being used. With a resonance-free hydraulic setup, the system can function in an optimum NVH.

Nomenclature

p: Dynamic pressure
V: Cylinder chamber fluid volume
t: Time
Q_r: Flow rate
Q_s: Volumetric losses
K: Fluid bulk modulus
A: Opening area
ρ: Density
ΔP: Pressure drop in an orifice
C_q: Maximum coefficient
λ: Flow number
d_h: Hydraulic diameter
ν: Poisson's ratio
K_d: Stiffness of the spring damper
C_d: Damper rating of the spring damper
J: Rotary inertia
E_p: The Young's modulus of the corresponding pressure
B_p: The bulk modulus of the corresponding pressure
f: Resonance frequency of a pipe
c_0: Speed of sound in a hydraulic oil
vol: Volume of the volumetric chamber
A_c: Area of the cross-section of a pipe
β_{eff}: Effective bulk modulus
β_{VG46}: Bulk modulus of VG46 oil
β_p: The pipe's wall bulk modulus
w_{comp}: Wall compliance of a pipe
r_o: Outer radius of a pipe
r_i: Inner radius of a pipe.

Data Availability

The experimental data that support this study's conclusions are made available upon request.

Disclosure

The project has been carried out within the activity of the laboratory Mechlav of the University of Ferrara.

Conflicts of Interest

The authors affirm that they have no known financial conflicts of interest or close relationships that could appear to have an influence on the work provided in this publication.

References

[1] D. Hill, *A History of Engineering in Classical and Medieval Times*, Routledge, Oxfordshire, 1996.

[2] L. Reti and F. di Giorgio Martini, "Francesco di Giorgio Martini's treatise on engineering and its plagiarists," *Technology and Culture*, vol. 4, no. 3, pp. 287–298, 1963.

[3] R. Agostino, "Le diverse et artificiose machine del capitano Agostino Ramelli dal ponte della Tresia," 1588.

[4] E. Mucchi, G. Dalpiaz, and A. Fernàndez del Rincòn, "Elastodynamic analysis of a gear pump. Part I: pressure distribution and gear eccentricity," *Mechanical Systems and Signal Processing*, vol. 24, no. 7, pp. 2160–2179, 2010.

[5] E. Mucchi, G. Dalpiaz, and A. Rivola, "Elastodynamic analysis of a gear pump. Part II: meshing phenomena and simulation results," *Mechanical Systems and Signal Processing*, vol. 24, no. 7, pp. 2180–2197, 2010.

[6] E. Mucchi and G. Dalpiaz, "Elasto-dynamic analysis of a gear pump–part III: experimental validation procedure and model extension to helical gears," *Mechanical Systems and Signal Processing*, vol. 50-51, pp. 174–192, 2015.

[7] E. Mucchi, G. Dalpiaz, and A. Fernàndez del Rincòn, "Elasto-dynamic analysis of a gear pump–part IV: improvement in the pressure distribution modelling," *Mechanical Systems and Signal Processing*, vol. 50-51, pp. 193–213, 2015.

[8] M. Battarra and E. Mucchi, "On the assessment of lumped parameter models for gear pump performance prediction," *Simulation Modelling Practice and Theory*, vol. 99, Article ID 102008, 2020.

[9] M. Battarra and E. Mucchi, "Analytical determination of the vane radial loads in balanced vane pumps," *Mechanism and Machine Theory*, vol. 154, Article ID 104037, 2020.

[10] Y. Hao, J. Hao, Z. Zuchao et al., "Review of the hydraulic and structural design of high-speed centrifugal pumps," *Frontiers in Energy Research*, vol. 10, Article ID 899093, 2022.

[11] A. H. Moghaddam, B. Kutschelis, F. Holz, T. Börjesson, and R. Skoda, "Three-dimensional flow simulation of a twin-screw pump for the analysis of gap flow characteristics," *Journal of Fluids Engineering*, vol. 144, no. 3, Article ID 031202, 2022.

[12] D. Yan, A. Kovacevic, Q. Tang, S. Rane, and W. Zhang, "Numerical modelling of twin-screw pumps based on computational fluid dynamics," *Proceedings of the Institution of Mechanical Engineers, Part C: Journal of Mechanical Engineering Science*, vol. 231, no. 24, pp. 4617–4634, 2017.

[13] X. Tong, H. Cao, M. Tao, and Y. Jiang, "Design and implementation of simulation operating system for screw pump removal rod," in *International Conference on Big Data, Electronics and Communication Engineering (BDECE 2019)*, vol. 94, pp. 134-135, Atlantis Press, 2019.

[14] R. Cieślicki and M. Karpenko, "An investigation of the impact of pump deformations on circumferential gap height as a factor influencing volumetric efficiency of external gear pumps," *Transport*, vol. 37, no. 6, pp. 373–382, 2022.

[15] S. H. Choudhari and M. V. Kharade, "Study and analysis of vibration characteristics of selected peristaltic pump," *International Journal of Science Technology & Engineering*, vol. 2, no. 11, pp. 852–855, 2016.

[16] G. J. Pagar and A. S. Nankar, "Vibration analysis of peristaltic pump using FEA and FFT analyzer," 2018.

[17] K. A. Harrison and K. A. Edge, "Reduction of axial piston pump pressure ripple," *Proceedings of the Institution of Mechanical Engineers, Part I: Journal of Systems and Control Engineering*, vol. 214, no. 1, pp. 53–64, 2000.

[18] J.-K. Kim, H.-E. Kim, J.-Y. Jung, S.-H. Oh, and S.-H. Jung, "Relation between pressure variations and noise in axial type oil piston pumps," *KSME International Journal*, vol. 18, pp. 1019–1025, 2004.

[19] L. Ericson, A. Johansson, and J.-O. Palmberg, "Noise reduction by means of non-uniform placement of pistons in an fluid power machine," in *Proceedings of the ASME 2009 Dynamic Systems and Control Conference. ASME 2009 Dynamic Systems and Control Conference*, pp. 381–388, ASME, Hollywood, California, USA, 2009.

[20] G. K. Seeniraj, M. Zhao, and M. Ivantysynova, "Effect of combining precompression grooves, PCFV And DCFV on pump noise generation," *International Journal of Fluid Power*, vol. 12, no. 3, pp. 53–63, 2011.

[21] P. Casoli, M. Pastori, F. Scolari, and M. Rundo, "Active pressure ripple control in axial piston pumps through high-frequency swash plate oscillations—a theoretical analysis," *Energies*, vol. 12, no. 7, Article ID 1377, 2019.

[22] T. Kim and M. Ivantysynova, "Active vibration/noise control of axial piston machine using swash plate control," in *Proceedings of the ASME/BATH 2017 Symposium on Fluid Power and Motion Control*, pp. 1–8, ASME, Sarasota, Forida, USA, 2017.

[23] T. R. Milind and M. Mitra, "A study on the dynamics and vibration behavior of an axial piston pump using combined MBD/FE approach," *Procedia Engineering*, vol. 144, pp. 452–460, 2016.

[24] W. Wang, "Vibration model and characteristic analysis of hydraulic piston pump," *Chemical Engineering Transactions*, vol. 59, pp. 61–66, 2017.

[25] Y. Pan, Y. Li, M. Huang, Y. Liao, and D. Liang, "Noise source identification and transmission path optimisation for noise reduction of an axial piston pump," *Applied Acoustics*, vol. 130, pp. 283–292, 2018.

[26] S. Ye, J. Zhang, B. Xu, L. Hou, J. Xiang, and H. Tang, "A theoretical dynamic model to study the vibration response characteristics of an axial piston pump," *Mechanical Systems and Signal Processing*, vol. 150, Article ID 107237, 2021.

[27] B. Xu, S. Ye, J. Zhang, and C. Zhang, "Flow ripple reduction of an axial piston pump by a combination of cross-angle and pressure relief grooves: analysis and optimization," *Journal of Mechanical Science and Technology*, vol. 30, no. 6, pp. 2531–2545, 2016.

[28] B. Xu, S.-G. Ye, and J.-H. Zhang, "Effects of index angle on flow ripple of a tandem axial piston pump," *Journal of Zhejiang University: Science A*, vol. 16, no. 5, pp. 404–417, 2015.

[29] X. Wu, C. Chen, C. Hong, and Y. He, "Flow ripple analysis and structural parametric design of a piston pump," *Journal of Mechanical Science and Technology*, vol. 31, no. 9, pp. 4245–4254, 2017.

[30] S.-G. Ye, J.-H. Zhang, and B. Xu, "Noise reduction of an axial piston pump by valve plate optimization," *Chinese Journal of Mechanical Engineering (English Edition)*, vol. 31, Article ID 57, 2018.

[31] P. Casoli, M. Pastori, and F. Scolari, "Swash plate design for pressure ripple reduction-a theoretical analysis," *AIP Conference Proceedings*, vol. 2191, Article ID 020038, 2019.

[32] F. Lyu, S. Ye, J. Zhang et al., "Theoretical and simulation investigations on flow ripple reduction of axial piston pumps using nonuniform distribution of pistons," *Journal of Dynamic Systems, Measurement, and Control*, vol. 143, no. 4, Article ID 041008, 2021.

[33] N. Bügener, J. Klecker, and J. Weber, "Analysis and improvement of the suction performance of axial piston pumps in swash plate design," *International Journal of Fluid Power*, vol. 15, no. 3, pp. 153–167, 2014.

[34] Y. Fang, J. Zhang, B. Xu et al., "Raising the speed limit of axial piston pumps by optimizing the suction duct," *Chinese Journal of Mechanical Engineering*, vol. 34, Article ID 105, 2021.

[35] Y. Wang, H. Dong, and Y. He, "A novel approach for predicting inlet pressure of aircraft hydraulic pumps under transient conditions," *Chinese Journal of Aeronautics*, vol. 32, no. 11, pp. 2566–2576, 2019.

[36] G. Pavić, "Vibroacoustical energy flow through straight pipes," *Journal of Sound and Vibration*, vol. 154, no. 3, pp. 411–429, 1992.

[37] F. Chevillotte, G. Pavić, G. Dubois, G. Proulx, and M. Gagnon, "Novel techniques for the analysis of dynamic pressure in penstocks," *IOP Conference Series: Earth and Environmental Science*, vol. 774, Article ID 012042, 2021.

[38] G. Pavić and F. Chevillotte, "Dynamic pressure propagation in pipes: modelling and measurment," The 18th International Conference on Fluid Flow Technologies, 2022.

[39] G. Pavić, "Acoustical analysis of pipes with flow using invariant field functions," *Journal of Sound and Vibration*, vol. 263, no. 1, pp. 153–174, 2003.

[40] G. Pavić, "Experimental identification of physical parameters of fluid-filled pipes using acoustical signal processing," *Applied Acoustics*, vol. 67, no. 9, pp. 864–881, 2006.

[41] M. Stosiak, M. Karpenko, O. Prentkovskis, A. Deptuła, and P. Skačkauskas, "Research of vibrations effect on hydraulic valves in military vehicles," *Defence Technology*, vol. 30, pp. 111–125, 2023.

[42] P. Gao, T. Yu, Y. Zhang, J. Wang, and J. Zhai, "Vibration analysis and control technologies of hydraulic pipeline system in aircraft: a review," *Chinese Journal of Aeronautics*, vol. 34, no. 4, pp. 83–114, 2021.

[43] B. Tuc, "The use of flexible hoses for reducing pressure ripple in hydraulic systems," 1981.

[44] J. Grabbel and M. Ivantysynova, "An Investigation of swash plate control concepts for displacement controlled actuators," *International Journal of Fluid Power*, vol. 6, no. 2, pp. 19–36, 2005.

[45] J. Ivantysyn and M. Ivantysynova, *Hydrostatic Pumps and Motors: Principles, Design, Performance, Modelling, Analysis, Control and Testing*, Tech Books International, 2003.

[46] P. K. Kalbfleisch and M. Ivantysynova, "Computational valve plate design in axial piston pumps/motors," *International Journal of Fluid Power*, vol. 20, pp. 177–208, 2019.

[47] R. Chacon and M. Ivantysynova, "Virtual prototyping of axial piston machines: numerical method and experimental validation," *Energies*, vol. 12, no. 9, Article ID 1674, 2019.

[48] P. Dudziński and A. Skurjat, "Impact of hydraulic system stiffness on its energy losses and its efficiency in positioning mechanical systems," *Energies*, vol. 15, no. 1, Article ID 294, 2022.